# THE APPLICATION OF WAVELET ANALYSIS FOR INTERNAL WAVE DETECTION IN SAR AND OPTICAL IMAGES DATA OVER TSUSHIMA STRAIT

YESSY ARVELYNA

**Abstract**

On this paper, wavelet analysis has been used for internal wave detection in ERS SAR and ASTER images data over Tsushima strait, southwest of Japan, during 1993-2004 period. Various wavelet transforms, such as Haar wavelet, Symlet wavelet, Coif wavelet, Daubechies wavelet, and Discreet Meyer wavelet, are tested comparably with different level of synthesize image on horizontal, diagonal, and vertical detail, and approximation to study the internal wave characteristic in image. Internal wave features were detected as elongated pattern in image with higher wavelet coefficient (>36) than sea surface (<10) on horizontal and vertical detail coefficient of image transforms at level 2-5. The decomposition image shows the tendency that the decomposition of internal wave feature using wavelet transform tends to follow the wavelet function. This may reduced the height of leading wave. Smoother result of internal wave shape can be formed using higher scale resolution of image and higher number of vanishing moments such as Daubechies wavelet-db5, Symlet wavelet-sym5, and Discrete Meyer wavelet. The compactly supported wavelet function with orthogonal basis with scale function and FIR filter, such as discrete Meyer function is proposed for smoothness of feature, space save coding, and to avoid depashing in image. So far, the detection processes were performed well on the internal waves data that occurred at north coast off Kitakyushu and NW/W/SW/E coast off Tsushima Island on June to September period whose lengths were detected between 6-28 km and wavelength between 120m-1.28km. The directions of internal wave propagation were varied between NW-SW at eastern channel and N-SW at western channel of Tsushima Strait.

*Keywords: wavelet analysis, SAR image, optical image, internal wave.*

## I. Introduction

The process in sea-air and atmosphere creates the oceanic phenomena. Oceanic phenomena, such as oceanic current, natural slick, and internal wave, are generated by eddy, bottom topography, and sea-air process. The oceanic features create signatures on sea surface, thus they can be detected in Synthetic Aperture Radar (SAR), and optical image in visible and short wave infrared channels, through dampening effect of small capillary Bragg waves, short sea surface wave within several cm. This process affects radar backscattering and changes the sun illumination; thus creates specific feature in SAR and optical image (Sabin, (1996)).

1 Tokyo Universily of Marine Science and Technology, Department of Marine Information System Engineering, 2-1-6 Hcchujima, Kolo-ku, Tokyo 135-8533, Japan. Email: yessy a@e.kaiyodai.ac.jp

Typically, oceanic features have different characteristics in image. Though in several cases they may appear look alike each other, such as sea surface signature of internal wave and sea surface wave, both appear as group of modulation pattern in SAR and optical image data. To handle this problem, pattern recognition of image can be used as an aid for automated classification of oceanic features in SAR and optical data. Compare to manual screening by an image analyst, an automated classification is the best tool in dealing with a huge satellite images data

On this paper, wavelet analysis has been used for internal wave detection in ERS SAR and ASTER images data over Tsushima Strait during 1993-2004 period. Tsushima Strait is located at northern side of the East China Sea, well known as a region where energy for exciting internal tides should be large (Baines, 1982). Internal tides over shelf break area, such ridges and sills, can generate the internal wave. The propagation of internal wave considerable velocity shear that can lead to turbulence and mixing, transport both mass and momentum, and create stormy current which imposes large stress on fishing ground, en route vessel, offshore oil drilling-rigs, etc (Alpers, (2002), Apel, (2002), Colosi et.al, (2001)). They are reflected on sea surface and have different characteristics with sea surface waves.

The numerical simulation shows that the energetic internal tides are generated over the continental shelf slope in the East China Sea. The $M_2$ mode conversion rate over south of Tsushima Strait and East China Sea was 41 GW (Niwa and Hibiya, (2001)). Tsushima Strait has strong tidal variability, maximum in summer 50 cm/s (Jacobs et.al, 2001). The strait has a depth of about 200m, a shallow water compare to the Japan Sea and the East China Sea.

The occurrences of the internal waves in Tsushima Strait and the Japan Sea have been mapped using ERS SAR and ASTER image data (Jackson, (2004)). Variety of internal wave signatures in the Eastern Channel of Tsushima Strait indicates a region of complex internal wave activity with a number of source locations. In situ observations of internal wave packets on the Korean Shelf in May 1999 show downward displacements of up to 26 meters of approximately 600m, speeds of 0.5 m/s, and time period between packets was 19 hours represent the generation by near-inertial internal waves (Kim et.al, (2001)). So far, the generation and the characteristics of the internal waves in Tsushima Strait have not been fully understand yet. This paper tried to analyze the internal wave detection method, characteristics and its generation using multi satellite observation.

## II. Review of Wavelet Analysis

Since oceanic features have different characteristic at various resolutions, it is necessary to process image into various resolutions which can be done by using different scale of processing. Certain function using Hilbert spaces can be broken into several basis functions, which can represent various scales (Prasad et al., 1997). Fourier analysis is an earliest technique of spectral analysis using trigonometric functions of various periods to represent functions at various scales. Since the Fourier transform is a function independent of time, the limitation of Fourier transform in locating feature varying with time is covered using window function technique, such as Gabor transform with Gaussian function. But still, time frequency window is rigid and does not vary over time. This lead into the application of wavelet transform which has capability in varying time and frequency windows by directly windowing the signal

and its Fourier transform, and by scaling window function appropriately to change its time window width.

The sea surface signature of internal waves are observed using backscatter information in ERS SAR image and sun illumination data in Visible and Near Infra Red Radiometer (VNIR), channel 520-860 nm, of ASTER image data (ERSDAC, (2003)). In SAR and optical image, generally the sea surface signature consists various features such as small gravity wave internal wave signature, and noise (Sabin, (1996)). Compare to small-scale gravity wave, sea surface signature of internal wave has enormous scales in length. Therefore the utilization of wavelet transform to detect internal wave feature in varying time with spatial analysis is proposed (Arvelyna et al, 2004).

Previous study applied Symlet wavelet to delineate internal wave features in ERS SAR image, which shown that wavelet function with higher number of vanishing moments or higher order polynomial, such as Symlet 8 (16 vanishing moments), smoothen internal wave feature, but decreasing the first crest wave height due to the shape of wavelet and scaling function. We assumed that other wavelet transform could delineate the internal wave features better. Therefore, in this paper various wavelet transforms, e.g. llaar wavelet, Symlet wavelet, Bi orthogonal wavelet. Coif wavelet, Daubechies wavelet, and Discreet Meyer wavelet, are tested comparably with different level of synthesize image on horizontal, diagonal, and vertical detail, and approximation to study the internal wave characteristic in image transform.

## III. Methodology

Wavelet analysis is performed by using multi resolution analysis of image for feature detection and image enhancement. Wavelet analysis performs local analysis to analyze a shorter region in image in time and scale data. Thus it allows more precise information than time and frequency region analysis such as Fourier analysis. The two-dimensional wavelet is defined as tensor products of one scaling function and three wavelets (Daubcchies, (1992)). Wavelet transform is applied with: (1) the scaling equation to define the multi resolution approximation of image by taking account the low intensities of image, and (2) wavelet function to define the details of image corresponds to the high intensities of image. The wavelet function and scaling function are described as follows,

$$\phi(x) = \sqrt{2}\sum_k h_k \phi(2x-k) \quad (1)$$

$$\psi(x) = \sqrt{2}\sum_k g_k \phi(2x-k) \quad (2)$$

where $\phi$ is the scaling function, $\psi$ is wavelet function, $h_k$ is scaling filter and $g_k = (-1)^k h_{1-k}$.

The discrete analysis is done with a successive process due to the type of wavelet transform for space-saving coding with sufficient synthesis. The representation of discrete analysis uses scale on dyadic bases from $2^1$, $2^2$,.., $2^n$ and each coefficient of j level is repeated $2^J$ times (Figure 1). At each level of processing, an approximation of image (cA), and deviation on horizontal (cD ), diagonal ($cD^h$) and vertical ($cD^v$) of image, are computed. High pass component (Hi_D) of decomposition characterizes the high frequency information is located using wavelet function, which acts as high pass filter with horizontal orientation. The low pass subimage (Lo_D) is computed by applying scaling function. The next scaling-level of processing is the sum of approximation and deviation of previous level. Then the resolution of image is increased as the scale of processing decreases and the detail the process of decomposition of image is described as follows,

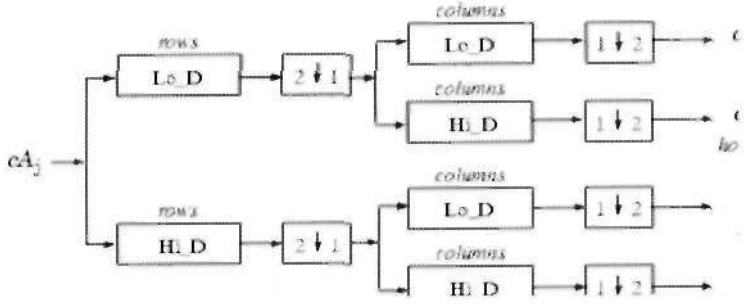


Figure 1. The basic decomposition and reconstruction steps for images (Misiti et al, (1996)).

where, [2|1| is downsample columns operation to keep the even indexed columns, FJ^ is downsample rows to keep the even indexed rows.

Several wavelets family functions are studied comparably, and for each wavelet function different resolution level are explored to detecting internal wave feature in image, as follows:

1. Orthogonal wavelets with Finite Impulse Response (FIR) filters. These wavelets can be defined through the scaling filter. Predefined families of such wavelets include Haar, Daubechies (dbN), Coiflets (coifN), and Symlets (SymN).
2. Biorthogonal wavelets with FIR filters. These wavelets have two scaling filters for reconstruction and decomposition respectively. The BiorSplines (biorN) wavelet family is a predefined family of this type.
3. Orthogonal wavelets without FIR filter, but with scale function. These wavelets are defined through wavelet function and scaling function. The Meyer wavelet family is a predefined family of this type.
4. Wavelets without FIR filter and without scale function. These wavelets are defined through the definition of the wavelet function, such as Morlet and Mexican hat.
5. Complex wavelets without FIR filter and without scale function. These wavelets can be defined through the definition of the wavelet function, such as Complex Gaussian and Shannon.

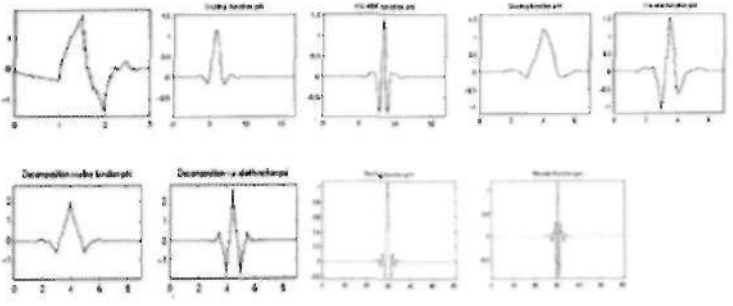

Figure2. Wavelet and scaling function: Daubechies wavelet (db2), Coiflet wavelet (coifJ), Symlet wavelet (sym4) (top, left to right), Biorthogonal wavelet (bior2.4), and Discrete Meyer wavelet (Daubechies, (1992)).

The applicationof FIR filters corresponding to compactly supported scaling function and orthonormal basis, which allows discrete wavelet analysis. Discrete analysis ensures space save coding and is sufficient for the synthesis. Several wavelet family functions consist vanishing moments (N), a characteristic of wavelet to suppress a polynomial function. Higher number of vanishing moments can smoothen out the wavelet function.

## IV. Results and Discussions

### 4.1 Internal Wave Observation

The circulation of internal wave modulates sea surface, increase/decrease radar backscatter or sun reflection as shown in vertical profile (Figure 4). The reflectance of crest increases about 20% in comparison with trough on visible channel. The profile of a train of internal waves composes a formation of several taller waves (crest), which the leading wave as the tallest one, and smaller depressed waves at one-third section. These conditions show that non-linier process was taking a part in transformation of internal tide into a train of independent solitary waves. When dispersive effect is negligible the leading part of waves amplified, then move faster than the depressed waves. As the dispersive effect is significant, the shape of wave turns into curvature (Zabusky et al., 1965). By looking at position of the leading wave, the propagation of the internal wave can be predicted.

The observation results show that internal waves were occurred at north coast off Kitakyushu and NW/W/SW/E coast off Tsushima Island on June to September period. The directions of internal wave propagation were varied between NW-SW at eastern channel and N-SW at western channel of Tsushima Strait (Table 1). The packet lengths are recorded between 7.5-9.4 km, crest lengths are 36.5-39.4 km, and wavelength of the leading wave between 330m-1.28 km. These results shown the internal waves in the Tsushima Strait possibly generated by different sources.

### 4.2 Internal Wave Detection Results

At original image, the internal wave signature forms elongated pattern at horizontal/vertical direction. As describe above, this form is resulted when dispersive effect taking account during internal wave propagation. Thus the reconstruction of horizontal/vertical wavelet coefficient of image can be used to detect internal wave clearly.

The detection results of internal wave thorough wavelet coefficient are presented using the profiles of transect along internal wave signature and three-dimensional profiles of original image. The reconstruction of horizontal coefficient, vertical transect and three dimensional profile of processed image at level 5 using various wavelet are shown in Figure 5 and Figure 6. The decomposition of Haar wavelet forms non-smooth profiles due to the usage of step function. But still, the crests can be detected in image. The dblO wavelet function creates smoother profile than Haar wavelet. The crests can be detected at values between 10-40. Small-scale gravity wave and regular sea surface were detected between 0-5. Higher vanishing moments applied by dblO tend to reduce the $2^{nd}$ and the $3^{rd}$ crest heights.

The decomposition image processed using Coiflet wavelet, coif5, attained maximum value at the middle of image, which has similarity with its wavelet function. Double vanishing moments of

Tabic I. Internal wave observation in ERS SAR and ASTER images data southwest coast of Japan during 1993-2004 period

| No | Location | **Path/Row** | **Date** | **Dir.** |
|---|---|---|---|---|
| *ERS SAR Images* | | | | |
| 1. | Nof'KK | 78/241 | 6/11/2000 | E |
| 2. | NofKK | 80/242 | 8/7/1994 | SE |
| 3 | NofKK | 80/243 | 8/7/1994 | E |
| 4 | NofKK | 80/244 | 8/7/1994 | SW |
| 5 | NofKK | 80/241 | 8/17/1993 | N |
| 6 | NofKK | 80/242 | 8/17/1993 | NW&NE |
| 7 | NofKK | 80/244 | 6/1/1995 | SW |
| 8 | EofTl | 81/242-243 | 8/1/1993 | SE |
| 9 | EofTI | 81/242-243 | 8/1/1993 | NE |
| 10 | EofTI | 81/243 | 8/1/1993 | SE |
| 11 | EofTI | 81/243 | 8/1/1993 | SE |
| 12 | EofTI | 81/243 | 8/29/1995 | SE |
| 13 | EofTI | 81/242 | 9/5/1993 | E |
| 14 | EofTI | 81/242 | 9/5/1993 | SE |
| 15 | EofTI | 81/243 | 9/5/1993 | SE |
| 16 | NW of TI | 82/242-243 | 6/3/1992 | SW |
| 17 | NWofTI | 82/243 | 7/9/1995 | SW |
| 18 | WofTI | 84/244 | 7/28/1995 | SW |
| 19 | WofTI | 84/243 | 6/30/1993 | SW |
| 20 | WofTI | 84/244 | 6/30/1993 | W |
| 21 | SW of TI | 82/244 | 7/9/1995 | SW |
| 22 | SW of TI | 82/244 | 7/9/1995 | SW |
| 23 | SW of TI | 84/244 | 6/30/1993 | NE |
| *ASTER Images Data* | | | | |
| 24 | SofTI | 114/105/6 | 5/1/2000 | NE |
| 25 | SofTI | 114/105/6 | 7/20/2000 | N |
| 26 | SEofTI | 114/106/6 | 7/4/2000 | NW |
| 27 | NEofTI | 114/106/6 | 7/4/2000 | SE |

(Note: TI = Tsushima Island; KK = Kitakyushu)

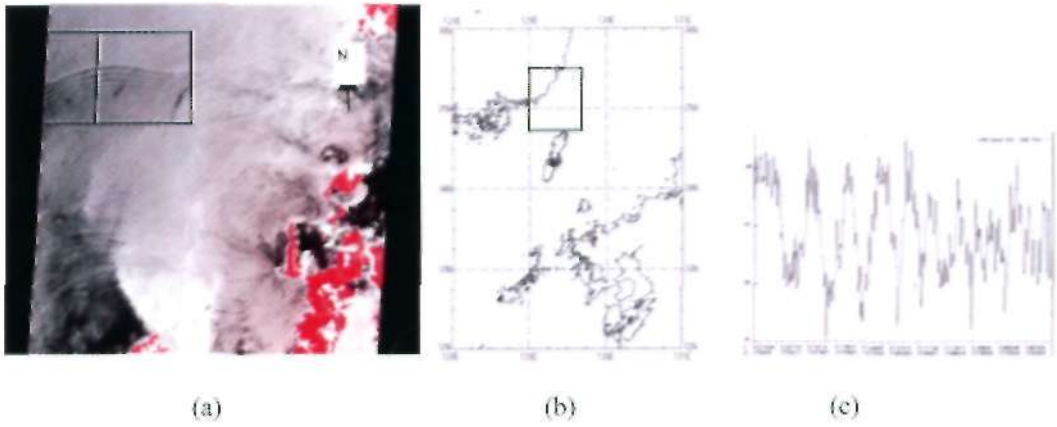


Figure 4. (a) Surface signature of internal wave in ASTER image data over south of the south west of Japan on 20-July-2000, Date: 11:32:14 JST (©METI/ERSDAC Japan), (b) map of study area over Tsushima Strait from ETOP02 data, (c) profile of sea surface reflectance on VNIR channel. The internal waves affect reflectance on sea surface. Crest increases reflectance about 20% in comparison with trough.

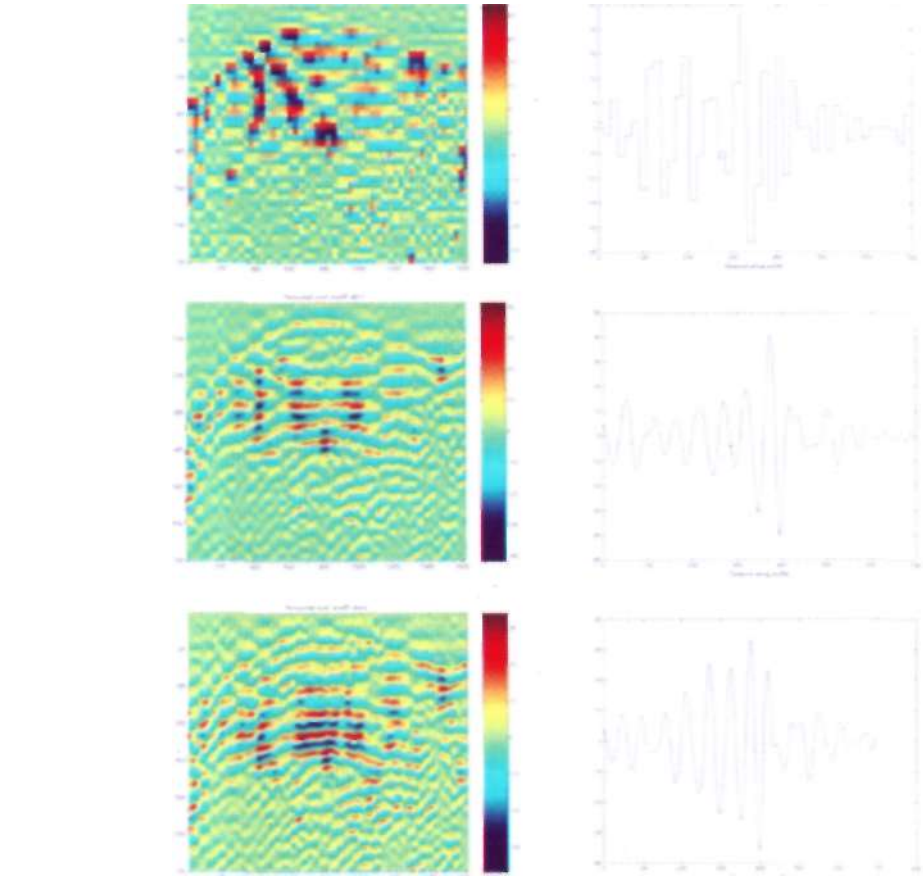

Figure 5.The reconstruction of approximation coefficient of image using Haar wavelet. Daubechies wavelet (db5) and Discrete Meyer wavelet at level 3, 4 and 5 (top to bottom).

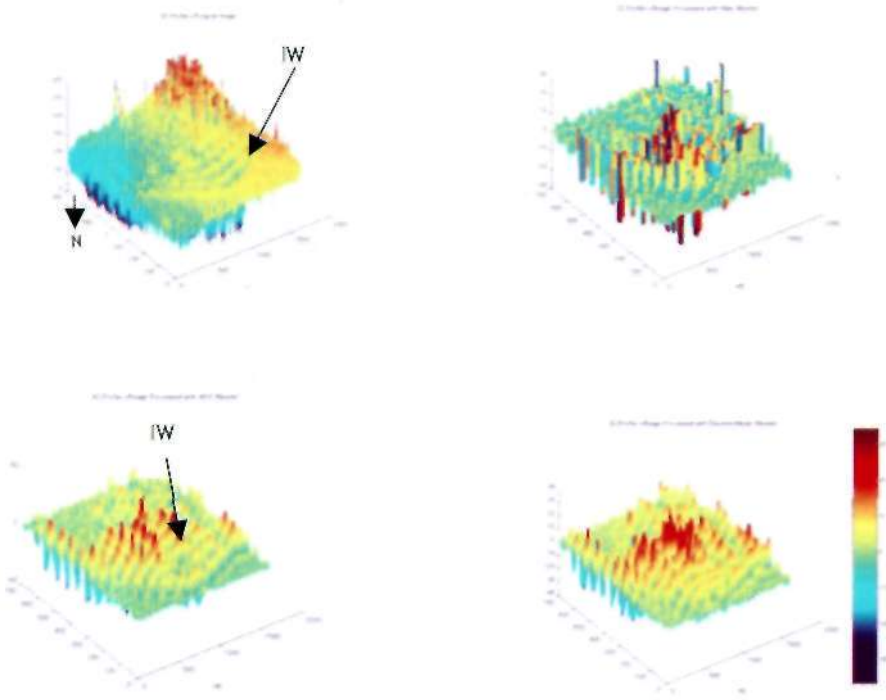


Figure 6. 3D profile of (a) original image, and horizontal coefficient of (a) using (b) Haar wavelet, (c) Daubechies wavelet (db5), and (d) Discrete Meyer wavelet at processing level-5.

Coiflet function tend to reduce crest height more than Daubechies wavelet. The profile of decomposition image by Symlet wavelet, sym8, has similarity with the result using dblO, since Symlet wavelet **adapts** Daubechies function. The symmetrical extension of Symlet wavelet formed higher crests than form created by dblO function. The decomposition result using bior6.8 has similarity with the results using sym8.

The usage of two FIR filters for decomposition slightly reduces crests height compare to previous result. The internal wave signature profiles using discrete Meyer wavelet perform the best result in detection. The crest height is maintained. Wavelet coefficients of internal waves are detected between 10-35. Strong crests value at the middle of image were formed as the effect of wavelet function. Trough and sea surface were detected at values between -10 to -50 and -5 to 5. Using horizontal decomposition of the first crest on level 1-5, the best correlation is attained by sym8 function. At high level, the coif5 tends to reduce crest height.

## V. **Conclusions**

Wavelet analysis has shown as useful tool in internal waves detection in SAR and optical image, by amplifying internal wave coefficient 2-5 times on high level processing of decomposition image (level 2-5), while reduced noise in image. The decomposition images show the tendency that the decomposition of internal

wave feature using wavelet transform tends to follow, trte Avavelet function. This may reduced the height of leading wave and increased the height of middle crest. Despite of these results, the application of wavelet transform... for internal wave detection has shown the capability in time and space analysis.

Smoother result of internal wave shape can be formed using higher scale resolution of image and higher number of vanishing moments such as db5, sym5, dmey. The compactly supported wavelet function with orthogonal basis[0] with scale function and FIR filter, such as discrete Meyer function is proposed for smoothness of feature, space save coding, and to avoid depashing in image.

For detail characteristics of the internal wave, the internal wave model in being investigated.

References


Alpers, W., Study of secondary internal wave generation by the interaction of an internal solitary wave with an underwater bank by using ERS SAR imagery and a numerical model, *Proceeding of Pan Ocean Remote Sensing Conference (PORSEC) 2002,* pp. 162-166, 2002.

Apel, J.R., Ostrovsky, L.A., and Stepanyants, Y.A., Internal solitons in the ocean. *Tech. Rep. MERCJRA0695. Milton S. Eisnhower Res. Center, Appl. Phys. Lab.,* The Johns Hopkins Univ. Laurel Maryland, 70, USA., 1995.

Arvelyna, Y., and Oshima, M., Application of wavelet transform for internal wave detection in SAR image. *International Journal of Remote Sensing and Earth Sciences,* 1(1), pp.58-85, 2004.

J.A., Beardsley, R.C, Lynch, J.F., Gawakiewicz, G., Chiu, C, and Scotti, A., Observation of nonlinear inernal waves on the outer New England Continental Shelf during summer shelfbreak primer study. *Journal of Geophysical Research,* 106(C5), pp. 9587-9601,2001.

Daubechies, I., *Ten Lectures on Wavelets,* CBMS-NSF, Pennsylvania, pp. 117-152, 1992.

ERSDAC, ASTER Products, Reference Guide, ERSDAC, 2003.

F. Sabins, *Remote Sensing: Principles and Interpretation,* W.H. Freeman & Co, 3rd Edition, pp.303, 1996.

Jackson, C.R., *An Atlas of Internal Solitary-like Waves and their Properties, Global Ocean Associates,* 2004.

Misiti, M., Oppenheim, G., and Poggi, J. M., *Wavelet Toolbox,* The Mathworks Inc., 1996.

Osborne, A.R., and Burch, T.L., Internal Solitons in the Andaman Sea, *Science,* 208, pp. 312-337, 1980.

Zabusky, Nj., Kruskal, M.D., Interaction of solitons in a collisionless plasma and the recurrcntce of initial plates, *Physics Review Letters,* 15, 243-250, 1965.